

# Hemispherical Harmonic Surface Description and Applications to Medical Image Analysis

Heng Huang  
Department of Computer Science  
Dartmouth College  
Hanover, NH, 03755

Lei Zhang, Dimitris Samaras  
Department of Computer Science  
SUNY at Stony Brook  
Stony Brook, NY, 11794

Li Shen  
Computer and Information Science  
Univ. of Mass. Dartmouth  
North Dartmouth, MA 02747

Fillia Makedon  
Department of Computer Science  
Dartmouth College  
Hanover, NH, 03755

Justin Pearlman  
Department of Cardiology  
Dartmouth Medical School  
Lebanon, NH 03756

## Abstract

*The use of surface harmonics for rigid and nonrigid shape description is well known. In this paper we define a set of complete hemispherical harmonic basis functions on a hemisphere domain and propose a novel parametric shape description method to efficiently and flexibly represent the surfaces of anatomical structures in medical images. As the first application of hemispherical harmonic theory in shape description, our technique differs from the previous surface harmonics shape descriptors, all of which don't work efficiently on the hemisphere-like objects that often exist in medical anatomical structures (e.g., ventricles, atriums, etc.). We demonstrate the effectiveness of our approach through theoretic and experimental exploration of a set of medical image applications. Furthermore, an evaluation criterion for surface modeling efficiency is described and the comparison results demonstrated that our method outperformed the previous approaches using spherical harmonic models.*

## 1. Introduction

Three dimensional (3D) shape description is a fundamental issue in 3D computer vision with many applications, such as shape registration, 3D object recognition and classification [1]. For a 3D object, its shape descriptor often consists of a set of parameters that can capture its shape information well. A global surface shape descriptor uses explicit or implicit functions to describe an entire surface shape into a small set of parameters, where every parameter affects the whole surface representation, not just local parts. As one important application in computer vision, medical image analysis also requires efficient and accurate shape descriptions. In particular many diseases resulting in or from

morphologic variations of structures (*e.g.*, heart, brain, *etc.*) shows the importance of analysis of shape variability for diagnostic classification and understanding of biomedical processes. There has been growing interest in shape description for medical applications [2]. Although, global surface description techniques have been proposed to address the biomedical anatomical structures reconstruction problems, different types of shape descriptors are needed due to the variety of different anatomical structures, *i.e.*, the previous surface harmonics shape descriptors cannot model the hemisphere-like objects efficiently. In this paper, we propose a novel global parametric surface description method that is in the form of linear combination of hemispherical basis functions. We examine the effectiveness of our approach through theoretic and experimental exploration of a set of medical image applications and demonstrate that our model works for simply connected objects and is especially suitable for hemisphere-like objects such as medical anatomical structures (ventricles, atriums, *etc.*).

In this paper, we apply our hemispherical harmonic shape description method on medical image analysis, however, our method is a general technique to be applied into many other areas in computer vision such as 3D face recognition, shape-based registration, *etc.*

### 1.1. Previous work

Many shape description methods and their applications in geodesy, biomedicine, molecular biology, and other fields have been explored [1]. Here we provide a summary of alternative approaches as context for our contribution.

Mathematically there are different methods of describing shapes including parametric models (such as harmonic functions [17], hyperquadrics [3], or superquadrics [4, 5]), medial axis (skeleton) [7, 8], distance distributions [6] and

landmark theory based descriptors [9]. Because spherical harmonic descriptions are smooth, accurate fine-scale shape representations with a sufficiently small approximation error [18], they are widely studied and used in different applications. In the shape matching field, Funkhouser and Kazhdan *et al.* [10, 11] proposed a rotation invariant spherical harmonic representation for 3D shapes to avoid the registration errors. Spherical harmonics also have a well-established standing in the molecular surfaces description and docking [13, 14]. Meanwhile many spherical harmonics based shape descriptions have been developed for medical image analysis [12]. For instance, in [15], Chen *et al.* presented their spherical harmonic model to analyze the left ventricular shape and motion. In [22], similarly, Edvardson and Smedby viewed a 3D object as a radial distance function on the unit sphere and tested their method on a data set from magnetic resonance imaging (MRI) of the brain. Matheny and Goldgof [16] used 3D and 4D surface harmonics to reconstruct rigid and nonrigid shapes. Because they used the radial surface function ( $r(\theta, \phi)$ ) in all models, their methods are limited to represent only star-shape or convex objects without holes.

Brechbühler *et al.* [17] presented an extended spherical harmonic (SPHARM) method to model any simply connected 3D object. A closed input object surface is assumed to be defined by a square surface parameter mesh converted from an isotropic voxel representation. The key component of this method is the mapping of surfaces of volumetric objects to parametrized surfaces prior to expansion into harmonics. SPHARM method have been applied in many medical imaging applications, *e.g.*, shape analysis of brain [19, 18] and cardiac [20, 21] structures. Since this method start the first order  $|Y_0^0(\theta, \phi)|$  from an ellipsoid, it is suitable to represent the surfaces with sphere topology, but not efficient in shape reconstruction of hemisphere-like objects.

In other research areas, spherical and hemispherical harmonics are widely used for representation of BRDFs (bi-directional reflectance distribution function), environment maps, illumination variation and image recognition [23, 24, 27], *etc.* Since they were applied on light/surface interaction models, their models used the radial surface function  $r(\theta, \phi)$ . Because our paper focuses on shape description, the review of these approaches is not provided.

## 1.2. Our contribution

As the first paper to introduce hemispherical harmonic theory into shape description, the contribution of this paper is to develop a set of complete hemispherical harmonic  $H_l^m(\theta, \phi)$  with shifted associated polynomials and prove their orthonormality property on a hemisphere domain. We propose the novel hemispherical harmonic surface description method to meet the requirement of surface reconstruction of hemisphere-like anatomical structures. Since our ba-

sis functions  $H_l^m(\theta, \phi)$  start from a hemisphere (order 0,  $|H_0^0(\theta, \phi)|$ ), our new method can represent the hemisphere-like objects efficiently by using less coefficients to describe the same surface. Furthermore, in order to evaluate the performance quantitatively, we provide a comparison criterion to the modeling efficiency and a shortcut to compute the modeling efficiency by using the hemispherical harmonic coefficients directly. The result of comparison with the previous SPHARM method shows our method outperformed the previous approaches. The applications are vast such as structures in cardiac MR image sequences [28]. Our method performing on the left ventricular surface reconstruction and shape sequence description is shown in section 3.

As a smooth and accurate fine-scale shape representation method, our hemispherical harmonic shape descriptors are useful in shape classification for statistical analysis of anatomical shape differences. Because we map the surfaces of voxel objects to parametrized surfaces before expansion into hemispherical harmonics, our method works well in simply connected objects (not only for star shapes). Since there is no shape descriptor for non-closed left ventricle in medical image analysis, some constraint rules were added into parametrization step to generate the shape descriptors for non-closed left ventricle or the other hemisphere-like anatomical structures. This non-closed shape representation is promising in the further shape analysis research.

This paper is organized as follows. Section 2 introduces the hemispherical harmonic basis functions and new surface description technique. Section 3 shows medical imaging applications to demonstrate our new surface descriptor. Section 4 evaluates its performance by comparing surface modeling efficiency with SPAHRM method. Section 5 concludes the paper.

## 2. Hemispherical harmonic shape descriptor

In this section, we first propose a set of new hemispherical harmonics (HemiSPHARM)  $H_l^m(\theta, \phi)$  and demonstrate their orthonormality property. We then describe our surface parametrization method that generates the HemiSPHARM shape description result. At last, we will evaluate the modeling efficiency of our HemiSPHARM description by comparing with spherical harmonics.

Previous SPHARM [17] represented the object surface as

$$\mathbf{v}(\theta, \phi) = \begin{pmatrix} x(\theta, \phi) \\ y(\theta, \phi) \\ z(\theta, \phi) \end{pmatrix}, \quad (1)$$

where  $\theta \in [0, \pi]$  is the polar angle and  $\phi \in [0, 2\pi]$  is the azimuthal angle. When the free variables  $\theta$  and  $\phi$  range over the whole sphere,  $\mathbf{v}(\theta, \phi)$  ranges over the whole object

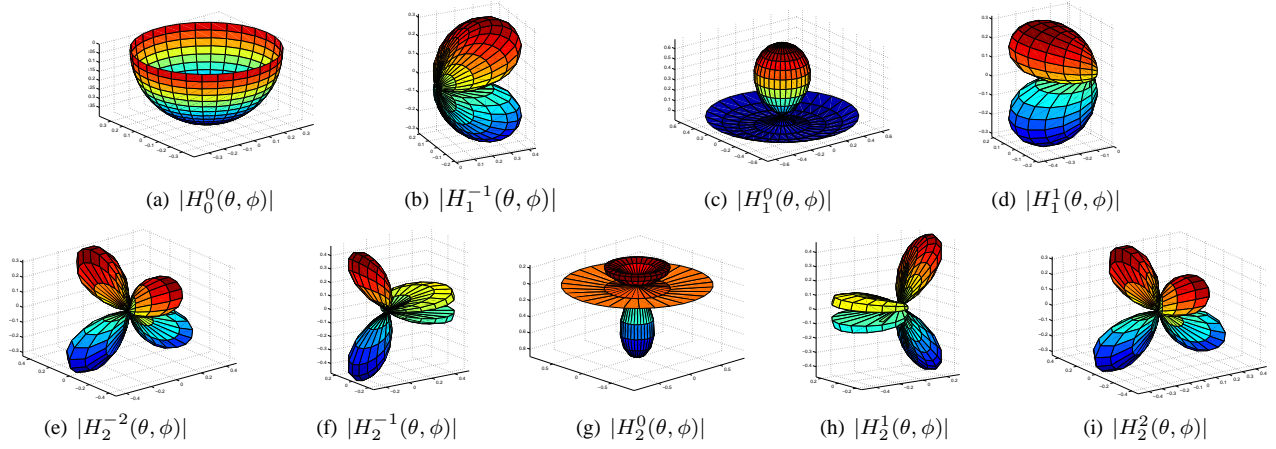


Figure 1: The visualization for hemispherical harmonics  $|H_l^m(\theta, \phi)|$ , for  $m = -l, \dots, l$ ,  $l = 0, 1, 2$ .

surface. The spherical harmonics expansion is used for all three coordinates and the surface  $\mathbf{v}(\theta, \phi)$  is expressed as a linear combination of spherical harmonic basis functions  $Y_l^m(\theta, \phi)$  of varying order  $l$  and degree  $m$ ,

$$\mathbf{v}(\theta, \phi) = \sum_{l=0}^{\infty} \sum_{m=-l}^l \mathbf{c}_l^m Y_l^m(\theta, \phi), \quad (2)$$

where

$$\mathbf{c}_l^m = (c_{lx}^m, c_{ly}^m, c_{lz}^m)^T. \quad (3)$$

The spherical harmonic basis functions are single-valued, smooth (infinitely differentiable), complex functions of  $(\theta, \phi)$ :

$$Y_l^m(\theta, \phi) = \sqrt{\frac{2l+1}{4\pi} \frac{(l-m)!}{(l+m)!}} P_l^m(\cos\theta) e^{im\phi}, \quad (4)$$

where  $P_l^m(\cos\theta)$  are associated Legendre polynomials (with argument  $\cos\theta$ ) that is defined by the differential equation

$$P_l^m(x) = \frac{(-1)^m}{2^l l!} (1-x^2)^{m/2} \frac{d^{m+l}}{dx^{m+l}} (x^2-1)^l, \quad (5)$$

where  $l$  and  $m$  are integers with  $-l \leq m \leq l$ . They are orthogonal over  $[-1, 1]$  with respect to  $l$  with the weighting function  $w(x) = 1$  [25]:

$$\int_{-1}^1 P_l^m(x) P_{l'}^m(x) dx = \frac{2(m+l)!}{(2l+1)(l-m)!} \delta_{ll'}. \quad (6)$$

The coefficients  $\mathbf{c}_l^m$  are 3D vectors. Their components,  $c_{lx}^m$ ,  $c_{ly}^m$ , and  $c_{lz}^m$  are usually complex numbers with a user-desired degree. These coefficients can be calculated by solving a set of linear equations in a least square fashion. As a result a set of coefficients is then used to express the surface in compact.

As an important property, the orthonormality property of spherical harmonic basis functions can be expressed as

$$\int_0^{2\pi} \int_0^\pi Y_l^m(\theta, \phi) \tilde{Y}_{l'}^{m'}(\theta, \phi) \sin\theta d\theta d\phi = \delta_{mm'} \delta_{ll'}. \quad (7)$$

Here,  $\tilde{z}$  denotes the complex conjugate and  $\delta_{ij}$  is the Kronecker delta:

$$\delta_{ij} \equiv \begin{cases} 0 & \text{for } i \neq j \\ 1 & \text{for } i = j \end{cases} \quad (8)$$

## 2.1. HemiSPHARM basis function

The standard definition of harmonic basis functions [24] starts from choosing the Legendre polynomials  $P_l(x)$  that satisfy the orthogonality relationship with the weight function  $w(x) = 1$ . Based on the unassociated Legendre polynomials  $P_l(x)$ , the associated Legendre polynomials  $P_l^m(x)$  are defined. At last the harmonics basis functions are constructed by combination of  $P_l^m(x)$  with  $\{\cos(m\phi), \sin(m\phi)\}$ .

As the first step in definition of HemiSPHARM we use the shifted Legendre polynomials [25] that are a set of functions analogous to the Legendre polynomials, but defined on the interval  $[-1, 0]$ . For Legendre polynomials  $P_l(x)$ , we use the linear transformation  $x = 2x' + 1$  to create the new polynomials:

$$\bar{P}_l(x') = P_l(2x' + 1). \quad (9)$$

From [26], for orthogonal polynomials  $P_l(x)$ , the linear transformation  $x = kx' + h$ ,  $k \neq 0$ , carries over the interval  $[a, b]$  into an interval  $[a', b']$  (or  $[b', a']$ ), and the weight function  $w(x)$  into  $w(kx' + h)$ . The polynomials  $(\text{sgn } k)^l |k|^{\frac{1}{2}} P_l(kx' + h)$  are also orthogonal on the interval

$[a', b']$  (or  $[b', a']$ ) with the weight function  $w(kx' + h)$ . Because  $x \in [-1, 1]$  in Legendre polynomials  $P_l(x)$ ,  $\bar{P}_l(x')$  are also orthogonal on the interval  $[-1, 0]$  with the weight function  $w(x) = 1$ . Thus, the orthogonal associated polynomials  $\bar{P}_l^m(x')$  are defined as:

$$\begin{aligned}\bar{P}_l^m(x') &= (-1)^m (1 - x'^2)^{m/2} \frac{d^m}{dx'^m} \bar{P}_l(x') \\ &= P_l^m(2x' + 1),\end{aligned}\quad (10)$$

and with respect to  $l$ ,

$$\int_{-1}^0 \bar{P}_l^m(x') \bar{P}_{l'}^m(x') dx' = \int_{-1}^0 P_l^m(2x'+1) P_{l'}^m(2x'+1) dx', \quad (11)$$

using Eq. (6),

$$\int_{-1}^0 \bar{P}_l^m(x') \bar{P}_{l'}^m(x') dx' = \frac{(m+l)!}{(2l+1)(l-m)!} \delta_{ll'} \quad (12)$$

Therefore, we get a set of orthogonal associated polynomials  $\bar{P}_l^m(\cos \theta)$  that are defined in the interval  $\theta \in [\frac{\pi}{2}, \pi]$ . Their relationship to associated Legendre polynomials is:

$$\bar{P}_l(\cos \theta) = P_l(2 \cos \theta + 1) \text{ on } \theta \in [\frac{\pi}{2}, \pi]. \quad (13)$$

Based on our shifted associated polynomials  $\bar{P}_l^m(\cos \theta)$ , we construct the HemiSPHARM basis functions  $H_l^m(\theta, \phi)$  as:

$$H_l^m(\theta, \phi) = \sqrt{\frac{2l+1}{2\pi} \frac{(l-m)!}{(l+m)!}} \bar{P}_l^m(\cos \theta) e^{im\phi}, \quad (14)$$

with  $\theta \in [\frac{\pi}{2}, \pi]$  and  $\phi \in [0, 2\pi)$ . Here, in order to keep the orthonormality of  $H_l^m(\theta, \phi)$ , we change the normalization value from

$$\sqrt{\frac{2l+1}{4\pi} \frac{(l-m)!}{(l+m)!}} \text{ to } \sqrt{\frac{2l+1}{2\pi} \frac{(l-m)!}{(l+m)!}}.$$

As a result,  $H_l^m(\theta, \phi)$  are orthogonal over  $[\frac{\pi}{2}, \pi] \times [0, 2\pi)$  with respect to both  $l$  and  $m$ :

$$\int_0^{2\pi} \int_{\frac{\pi}{2}}^{\pi} H_l^m(\theta, \phi) \tilde{H}_{l'}^{m'}(\theta, \phi) \sin \theta d\theta d\phi = \delta_{mm'} \delta_{ll'}. \quad (15)$$

Figure 1 shows the visualization of HemiSPHARM basis functions for  $l = 0, 1, 2$  and  $m = -l, \dots, l$ .

## 2.2. Surface parametrization

In order to describe a voxel surface (figure 2(b)) using HemiSPHARM, we first need to create a continuous and uniform mapping from the object surface (see figure 2(c)) to the surface of a half unit sphere (see figure 2(d)) so that each vertex on the object surface can be assigned a pair

of spherical coordinates  $(\theta, \phi)$  in figure 2(a). This process is called *surface parameterization*, and the surface of the half unit sphere becomes our parameter space. We employ a hemispherical parameterization approach that is similar to the spherical parameterization approach proposed by Brechbühler *et al.* [17] to exploit a square surface mesh.

The parameterization is constructed by creating a harmonic map from the object surface to the parameter surface. For colatitude  $\theta$  two poles are selected in the surface mesh by finding the two vertices with the maximum (for the hemisphere-like object, it should be the center of top slice which includes many points with the same or close maximum  $z$  values, *e.g.*, our parametrization for left ventricular surface) and minimum  $z$  coordinate in object space. Then, a Laplace equation (Eq. (16)) with Dirichlet conditions (Eq. (17) and Eq. (18)) is solved for colatitude  $\theta$ :

$$\nabla^2 \theta = 0 \text{ (except at the poles)} \quad (16)$$

$$\theta_{north} = \frac{\pi}{2} \quad (17)$$

$$\theta_{south} = \pi \quad (18)$$

Since our case is discrete, we can approximate Eq. (16) by assuming that each vertex's colatitude (except at the poles) equals the average of its neighbours' colatitudes. Thus, after assigning  $\theta_{north} = \frac{\pi}{2}$  to the north pole and  $\theta_{south} = \pi$  to the south pole, we can form a system of linear equations by considering all the vertices and obtain the solution by solving this linear system. For longitude  $\phi$  the same approach can be employed except that longitude is a cyclic parameter. To overcome this problem, a "date line" is introduced. When crossing the date line, longitude is incremented or decremented by  $2\pi$  depending on the crossing direction. After slightly modifying the linear system according to the date line, the solution for longitude  $\phi$  can also be achieved.

## 2.3. Surface description

The parameterization result is a bijective mapping between each vertex  $\mathbf{v} = (x, y, z)^T$  on a surface and a pair of spherical coordinates  $(\theta, \phi)$  ( $\theta \in [\frac{\pi}{2}, \pi]$ ,  $\phi \in [0, 2\pi)$ ). We use  $\mathbf{v}(\theta, \phi)$  to denote such a mapping, meaning that, according to the mapping,  $\mathbf{v}$  is parameterized with the spherical coordinates  $(\theta, \phi)$ . Taking into consideration the  $x$ ,  $y$ , and  $z$  coordinates of  $\mathbf{v}$  in object space, the mapping can be represented as:

$$\mathbf{v}(\theta, \phi) = \begin{pmatrix} x(\theta, \phi) \\ y(\theta, \phi) \\ z(\theta, \phi) \end{pmatrix}. \quad (19)$$

We use the surface net representation to expand the surface of object into our HemiSPHARM basis functions with

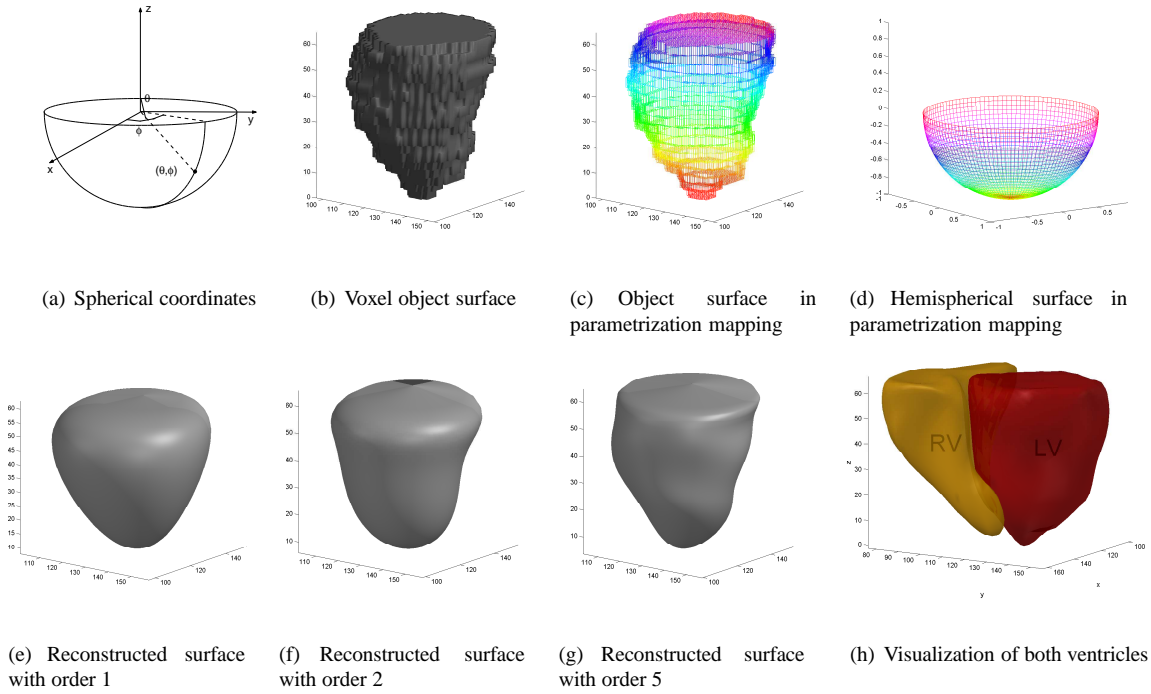


Figure 2: Surface parametrization and reconstruction. (a) shows the spherical coordinates  $(\theta, \phi)$ ; (b) shows the voxel surface of left ventricle before surface reconstruction; (c) and (d) show the parametrization mapping from the object surface (c) to the surface of a half unit sphere (d); (e)-(g) show the reconstructed surfaces of left ventricle with order 1, 2, 5 respectively; (h) shows the reconstructed results of both ventricular (right and left) surfaces.

the coefficients  $\mathbf{c}_l^m = (c_{lx}^m, c_{ly}^m, c_{lz}^m)^T$ :

$$\mathbf{v}(\theta, \phi) = \begin{pmatrix} x(\theta, \phi) \\ y(\theta, \phi) \\ z(\theta, \phi) \end{pmatrix} = \sum_{l=0}^{\infty} \sum_{m=-l}^l \mathbf{c}_l^m H_l^m(\theta, \phi) \approx \sum_{l=0}^L \sum_{m=-l}^l \mathbf{c}_l^m H_l^m(\theta, \phi), \quad (20)$$

where  $L$  is used to truncate the series into a desired finite number of terms. Figure 2(g) shows the reconstructed surface result of voxel object in figure 2(b). The coefficients are calculated by forming the inner product of  $\mathbf{v}$  with the HemiSPHARM basis functions:

$$\begin{aligned} \mathbf{c}_l^m &= \langle \mathbf{v}(\theta, \phi), H_l^m(\theta, \phi) \rangle \\ &= \int_{\frac{\pi}{2}}^{\pi} \int_0^{2\pi} \mathbf{v}(\theta, \phi) H_l^m(\theta, \phi) d\phi \sin \theta d\theta. \end{aligned} \quad (21)$$

### 3. Medical applications of HemiSPHARM shape descriptors

In this section we will describe how to apply our HemiSPHARM shape descriptors into shape analysis in medical image analysis applications. Based on segmented image

data of medical anatomical structures, we use the HemiSPHARM method explained above for surface reconstruction and our novel shape description allows researchers to perform further shape analysis or classification and access more functional details. In the following, we describe how the HemiSPHARM shape descriptors can help the medical applications in details.

#### 3.1. Surface reconstruction in cardiac MRI

Visualization and modeling of cardiac shapes can provide direct and reliable indicators of cardiac function [28]. Since the shapes of hearts and ventricles are close to hemiellipsoid, it's intuitive to apply our HemiSPHARM descriptors to describe their shapes. Furthermore, in section 4, we will demonstrate that our description is more efficient than previous SPHARM method in hemisphere-like shape modeling. By using the segmented cardiac MRI data, the HemiSPHARM model can accurately visualize cardiac or ventricle geometry and function and provide the shape descriptors.

Figure 2(e), 2(f), 2(g) show the surface reconstruction result of left ventricle which is the most important functional structure in cardiac studies. By increasing the value of order  $l$  from 1, 2 to 5, a more detailed surface is created. Meanwhile we reconstructed both ventricular (right and left) surfaces and the result is shown in figure 2(h).

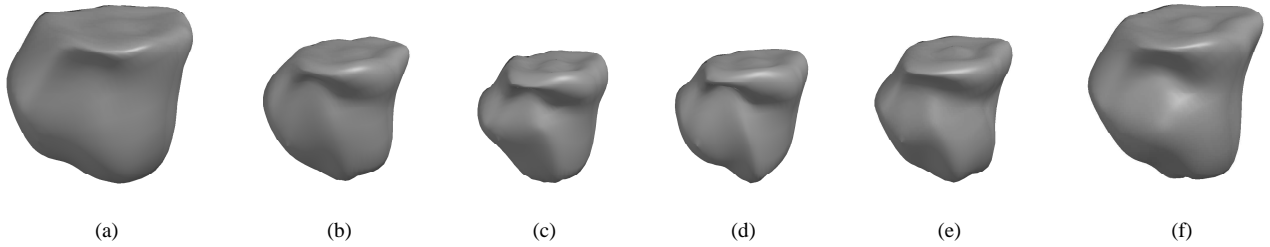


Figure 3: The visualization result of shape sequence of a left ventricular inner surface during one heart cycle. The shapes change from a diastolic phase (with largest volume) to next diastolic phase and the middle ones lie close to the systolic phase (with smallest volume).

This new surface description method also provides a promising visualization and representation method for studying spatio-temporal cardiac structures. For a beating heart, each surface model during a heart cycle can be generated by HemiSPHARM method and a set of surfaces sequence can describe the heart contraction and dilation in every direction of 3D space. Based on this shape sequence visualization result, more valuable diagnostic and prognostic information can be derived for helping make clinical determinations. Figure 3 describes a shape sequence reconstruction result of a left ventricular inner surface during one heart cycle. The shapes change from a diastolic phase (with largest volume) to next diastolic phase and the middle ones lie close to the systolic phase (with smallest volume).

### 3.2. Surface reconstruction for non-closed objects

During cardiac shape analysis study, since the ventricles and atriums are open objects, people only need the surface descriptions without the top parts. But the traditional spherical harmonics methods work only for closed surface. Thus, the closed shape descriptions introduce errors into shape analysis and classification for cardiac shape studies. In order to solve this problem, we added constraint rules into the surface parametrization step presented in section 2.2: 1) the points on the boundary of top slice (see figure 2(b)) are parametrized as  $[\pi/2, \phi]$ ; 2) the apex point of ventricle is parametrized as  $[\pi, \phi]$ . The new parametrization result is shown in figure 4(a) and the surface reconstruction results are shown in figure 4(b).

After removing the top parts, these non-closed shape descriptors are more accurate in the left ventricular shape representation than the closed description method. They can provide more functional shape information for cardiac shape analysis.

## 4. Modeling efficiency analysis

In this section, we show the modeling efficiency (or accuracy) of our HemiSPHARM description by comparing to

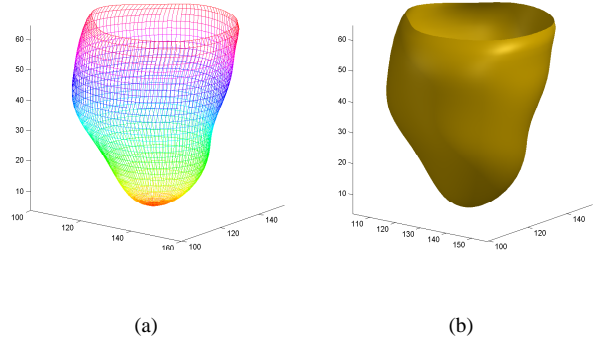


Figure 4: (a) shows the new parametrized surface for non-closed shape representation; (b) shows the reconstruction results for non-closed left ventricular surface.

the previous method. Since the methods [12, 15, 22, 16] that did harmonics expansion without mapping the surface of volumetric object to parametrized surface can only work on the star shape, we compare our method to the SPHARM method proposed by Brechbühler *et al.* [17] on single connected objects.

In order to analyze the number of required coefficients, we use the energy fraction to determine the captured energy by a given number of coefficients:

$$\begin{aligned} \text{Modeling Efficiency} &= \frac{E_L}{E} \\ &= \frac{\sum_{l=0}^L \sum_{m=-l}^l (|c_{lx}^m|^2 + |c_{ly}^m|^2 + |c_{lz}^m|^2)}{\int_0^{2\pi} \int_{\frac{\pi}{2}}^{\pi} \mathbf{v}(\theta, \phi)^2 \sin \theta d\theta d\phi} \end{aligned}$$

When the centroids of objects are moved to the origin, we can compute the energy  $E$  in the definition of modeling efficiency (or accuracy) as follows (it is different to the previous definition in [27], because their definition only work

for radial surface function based spherical harmonics):

$$\begin{aligned}
E &= \int_0^{2\pi} \int_{\frac{\pi}{2}}^{\pi} \mathbf{v}(\theta, \phi)^2 \sin \theta d\theta d\phi \\
&= \int_0^{2\pi} \int_{\frac{\pi}{2}}^{\pi} \left( \sum_{f \in \{x,y,z\}} f(\theta, \phi)^2 \sin \theta d\theta d\phi \right) \\
&= \sum_{f \in \{x,y,z\}} \left( \int_0^{2\pi} \int_{\frac{\pi}{2}}^{\pi} f(\theta, \phi)^2 \times \sin \theta d\theta d\phi \right) \\
&= \sum_{f \in \{x,y,z\}} \left( \int_0^{2\pi} \int_{\frac{\pi}{2}}^{\pi} \left( \sum_{l=0}^L \sum_{m=-l}^l c_{lf}^m H_l^m(\theta, \phi) \right) \right. \\
&\quad \left. \times \sum_{l=0}^L \sum_{m=-l}^l c_{lf}^m H_l^m(\theta, \phi) \sin \theta d\theta d\phi \right) \quad (22)
\end{aligned}$$

By the orthonormality property of HemiSPHARM basis functions Eq. (15),

$$\begin{aligned}
\int_0^{2\pi} \int_{\frac{\pi}{2}}^{\pi} \mathbf{v}(\theta, \phi)^2 \sin \theta d\theta d\phi &= \sum_{l=0}^{\infty} \sum_{m=-l}^l (|c_{lx}^m|^2 + |c_{ly}^m|^2 + |c_{lz}^m|^2) \\
&> \sum_{l=0}^L \sum_{m=-l}^l (|c_{lx}^m|^2 + |c_{ly}^m|^2 + |c_{lz}^m|^2).
\end{aligned}$$

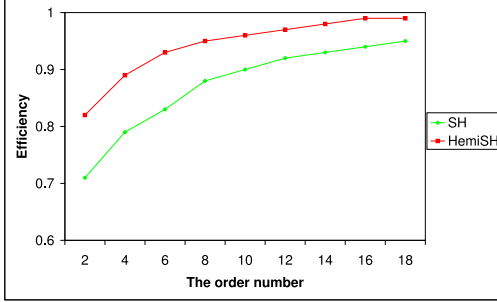


Figure 5: The comparison result of modeling efficiency between the HemiSPHARM description and SPHARM method in our experiment (left ventricle surface reconstruction is used in comparison). The red line represents the HemiSPHARM modeling efficiency and the green line represents SPHARM method. The  $x$ -axis is the values of order  $l$ .

Obviously if we increase the order number  $L$ , the modeling efficiency towards to 1. Figure 5 shows the comparison result of modeling efficiency between the HemiSPHARM description and SPHARM method in our experiment (left ventricle surface reconstruction is used with red line representing the HemiSPHARM modeling efficiency and green

line representing SPHARM). Because our HemiSPHARM basis functions start from a hemisphere (see Figure 1(a)) and the SPHARM basis functions start from sphere, HemiSPHARM method can describe the hemisphere-like objects more efficiently. In other words, HemiSPHARM requires fewer coefficients (less order  $l$ ) than SPHARM to describe the same surfaces of hemisphere-like objects.

## 5. Conclusion and future work

The contribution of this paper is a novel shape description method for the requirement of surface reconstruction for hemisphere-like anatomical structures. In order to propose the new shape descriptors, we use a set of new orthogonal associated polynomials to generate the orthonormal hemispherical harmonics  $H_l^m(\theta, \phi)$ . The hemispherical harmonics are defined on a hemisphere domain and we map the surfaces of volumetric objects to parametrized surfaces prior to expansion into hemispherical harmonics. The success of the algorithm is in its modeling efficiency by using fewer coefficients than previous spherical harmonic method to represent the same surface. The surface reconstruction results of using segmented cardiac MRI clearly demonstrate the effectiveness of our shape description method. Our new method is a general technique and can be applied into shape matching, 3D face recognition, molecular surfaces registration and docking, or other research fields in computer vision.

There are several opportunities for future work on this novel method. One of our future works is focused on adding the optimized surface parametrization step to perform the equal area mapping for parametrizing the volumetric objects. The shape representation for non-closed simple connected objects provides promising shape descriptors for the further shape analysis. Another research direction can be the left ventricle shape classification for cardiac functional analysis on shape differences.

## References

- [1] S. Loncaric, "A survey of shape analysis techniques," *Pattern Recognition*, Vol. 31(8), pp. 983–1001, 1998.
- [2] VALENTÍN MASERO and JUAN M. LEÓN-ROJAS and JOSÉ MORENOa, "Volume Reconstruction for Health Care A Survey of Computational Methods," *Annals of the New York Academy of Sciences*, Vol. 980, pp. 198–211, 2002.
- [3] Andrew J. Hanson, "Hyperquadrics: smoothly deformable shapes with convex polyhedral bounds," *Comput. Vision Graph. Image Process.*, Vol. 44(2), pp. 191–210, 1988.
- [4] F. Solina and R. Bajcsy, "Recovery of Parametric Models from Range Images: The Case for Superquadrics with Global

- Deformations,” *IEEE Trans. Pattern Anal. Mach. Intell.*, Vol. 12(2), pp. 131–147, 1990.
- [5] Demetri Terzopoulos and Dimitri Metaxas, “Dynamic 3D Models with Local and Global Deformations: Deformable Superquadrics,” *IEEE Trans. Pattern Anal. Mach. Intell.*, Vol. 13(7), pp. 703–714, 1991.
- [6] M. Leventon and W. Grimson and O. Faugeras, “Statistical Shape Influence in Geodesic Active Contours,” *Proc. of IEEE Conf. Computer Vision and Pattern Recognition*, pp. 316–323, 2000.
- [7] Jules Bloomenthal and Chek Lim, “Skeletal Methods of Shape Manipulation,” *Proceedings of the International Conference on Shape Modeling and Applications*, pp. 44–47, 1999.
- [8] Duane W. Storti and George M. Turkiyyah and Mark A. Gantner and Chek T. Lim and Derek M. Stal, “Skeleton-based modeling operations on solids,” *Proceedings of the fourth ACM symposium on Solid modeling and applications*, pp. 141–154, 1997.
- [9] F. Bookstein, “Landmark methods for forms without landmarks: morphometrics of group differences in outline shape,” *Medical Image Analysis*, Vol. 1(2), pp. 225–243, 1996.
- [10] Thomas Funkhouser and Patrick Min and Michael Kazhdan and Joyce Chen and Alex Halderman and David Dobkin and David Jacobs, “A search engine for 3D models,” *ACM Trans. Graph.*, Vol. 22(1), pp. 83–105, 2003.
- [11] Michael Kazhdan and Thomas Funkhouser and Szymon Rusinkiewicz, “Rotation invariant spherical harmonic representation of 3D shape descriptors,” *Proceedings of the 2003 Eurographics/ACM SIGGRAPH symposium on Geometry processing*, pp. 156–164, 2003.
- [12] G. Burel and H. Henocq, “Determination of the Orientation of 3D Objects Using Spherical-Harmonics,” *Graphical Models and Image Processing*, Vol. 57(5), pp. 400–408, 1995.
- [13] W. Cai and X. Shao and B. Maigret, “Protein-ligand recognition using spherical harmonic molecular surfaces: towards a fast and efficient filter for large virtual throughput screening,” *J Mol Graph Model.*, Vol. 20(4), pp. 313–328, 2002.
- [14] D.W. Ritchie and G.J. Kemp, “Protein docking using spherical polar Fourier correlations,” *Proteins*, Vol. 39(2), pp. 178–194, 1999.
- [15] C. W. Chen and T. S. Huang and M. Arrott, Modeling, analysis, and visualization of left ventricle shape and motion by hierarchical decomposition, *IEEE Transactions on Pattern Analysis and Machine Intelligence*, Vol. 16(4), pp. 342–356, 1994.
- [16] A. Matheny and D.B. Goldgof, “The use of three- and four-dimensional surface harmonics for rigid and nonrigid shape recovery and representation,” *IEEE Transactions on Pattern Analysis and Machine Intelligence*, Vol. 17(10), pp. 967–981, 1995.
- [17] Ch. Brechbühler and G. Gerig and O. Kübler, “Parametrization of closed surfaces for 3D shape description,” *Computer Vision and Image Understanding*, Vol. 61(2), pp. 154–170, 1995.
- [18] M. Styner and G. Gerig, “Three-Dimensional Medial Shape Representation Incorporating Object Variability,” *Proc. of IEEE Conf. Computer Vision and Pattern Recognition*, pp. 651–656, 2002.
- [19] G. Gerig and M. Styner, “Shape versus Size: Improved Understanding of the Morphology of Brain Structures,” *Proc. of In. Conf. on Medical Image Computing and Computer Assisted Intervention, LNCS 2208*, pp. 24–32, 2001.
- [20] H. Huang and L. Shen and R. Zhang and F. Makedon and B. Hettelman and J. D. Pearlman, “Surface Alignment of 3D Spherical Harmonic Models: Application to Cardiac MRI Analysis,” *Proc. of In. Conf. on Medical Image Computing and Computer Assisted Intervention, LNCS 3749*, pp. 67–74, 2005.
- [21] H. Huang and L. Shen and R. Zhang and F. Makedon and B. Hettelman and J. D. Pearlman, “A Prediction Framework for Cardiac Resynchronization Therapy Via 4D Cardiac Motion Analysis,” *Proc. of In. Conf. on Medical Image Computing and Computer Assisted Intervention, LNCS 3749*, pp. 704–711, 2005.
- [22] H. Edvardson and O. Smedby, “Compact and efficient 3D shape description through radial function approximation,” *Comput Methods Programs Biomed.*, Vol. 72(2), pp. 89–97, 2003.
- [23] Pascal Gautron and Jaroslav Křivánek and Sumanta N. Pattanaik and Kadi Bouatouch, “A Novel Hemispherical Basis for Accurate and Efficient Rendering,” *Rendering Techniques 2004, Eurographics Symposium on Rendering*, pp. 321–330, 2004.
- [24] Oleg A. Makhotkin, “Analysis of Radiative Transfer Between Surfaces by Hemispherical Harmonics,” *Journal of Quantitative Spectroscopy and Radiative Transfer*, Vol. 56(6), pp. 869–879, 1996.
- [25] Eric Weisstein, “World of Mathematics: A Wolfram Web Resource,” <http://mathworld.wolfram.com/LegendrePolynomial.html>, 2004.
- [26] Gabor Szegő, “Orthogonal polynomials,” *American Mathematical Society, Providence, Rhode Island*, pp. 29, 1975.
- [27] Ravi Ramamoorthi and Pat Hanrahan, “Frequency space environment map rendering,” *Proceedings of SIGGRAPH*, pp. 517–526, 2002.
- [28] A.F. Frangi and W.J. Niessen and M.A. Viergever, “Three-dimensional modeling for functional analysis of cardiac images: a review,” *IEEE Transactions on Medical Imaging*, Vol. 20(1), pp. 2–25, 2001.